

## Fluorescence of tin-sensitized manganese in single-crystalline NaCl

A. Muñoz F. and J. Rubio O.

*Departamento de Física, Universidad Autónoma Metropolitana-Iztapalapa, Apartado Postal 55-534, 09340 México, Distrito Federal, Mexico*

(Received 18 September 1987; revised manuscript received 24 May 1988)

Energy transfer from  $\text{Sn}^{2+}$  to  $\text{Mn}^{2+}$  ions has been investigated in single crystals of NaCl slightly doped with tin and manganese ions. The data obtained indicate that the tin-sensitized manganese fluorescence which takes place in our doubly doped quenched crystals occurs between the Sn-Mn pairs which are preferentially formed in the crystalline matrix. The essential features of the kinetics of  $\text{Sn}^{2+} \rightarrow \text{Mn}^{2+}$  energy transfer are described considering an energy-level system in which both the sensitizer and activator ions are treated as two energy-level systems. From the solutions of the rate equations describing the time evolution of the excited-state populations for the isolated Sn and the Sn-Mn complex and our experimentally determined data, the rate of  $\text{Sn}^{2+} \rightarrow \text{Mn}^{2+}$  energy transfer was estimated to be greater than  $7 \times 10^8 \text{ s}^{-1}$ . This value was then compared with those calculated with use of Dexter's theory of energy transfer via either multipolar- or exchange-interaction mechanisms. To do this, several configurations for the Sn-Mn pair complex were employed. These calculations allowed us to get some insight into the possible nature of the tin-manganese complex and to establish that the experimental data can only be plausibly explained if a short-range interaction mechanism for energy transfer is active between these two impurity ions. Moreover, from the solution of the rate equations for the steady-state case, the ratio of the number of coupled  $\text{Sn}^{2+}$  ions which transfer energy to  $\text{Mn}^{2+}$  to the total number of tin ions in the samples was estimated to be approximately 5%. This result gives support to the ionic-radius criterion proposed by Rubio and co-workers to predict pairing between two doubly valent impurity ions in an alkali halide host between which energy transfer is desired.

### I. INTRODUCTION

Recently, energy transfer from  $\text{Eu}^{2+}$  to  $\text{Mn}^{2+}$  ions was analyzed by Shinn and Sibley<sup>1</sup> in monocrystalline  $\text{RbMgF}_3:\text{Eu,Mn}$ . It was found that the energy transfer was so efficient even at low dopant concentrations that it should have occurred between the copious Eu-Mn pairs which were preferentially formed in the lattice.

Motivated by this uncommon situation Rubio and co-workers<sup>2-5</sup> later studied the energy transfer from europium or lead to manganese ions in monocrystalline NaCl, NaBr, and KCl. As in  $\text{RbMgF}_3:\text{Eu,Mn}$  the energy transfer was found to occur even for a very low concentration of either the sensitizer and/or the activator ions. From this fact and other experimental data it was inferred that the energy transfer could not take place between sensitizers and activators randomly distributed in the lattice. Rather, it occurred between the Eu-Mn and Pb-Mn pairs which were preferentially formed in the alkali halide matrix; the number of these pairs being, however, strongly dependent on the type of selected host. In fact, these pairs are more numerous in the sodium halides than in the potassium halides. This pairing between impurities most likely occurs to reduce the strain in the lattice which results from the introduction of either impurity alone.

In order to explain the observed tendency for impurity pairing, Rubio *et al.*<sup>2-5</sup> pointed out that both Eu-Mn and

Pb-Mn pairs might be expected to occur in both NaCl and NaBr in view of the ionic radii of the  $\text{Eu}^{2+}$  (1.12 Å),  $\text{Pb}^{2+}$  (1.24 Å), and  $\text{Mn}^{2+}$  (0.80 Å) ions. In fact, if either Eu-Mn or Pb-Mn ions couple through a  $\text{Cl}^-$  ion along the [100] direction, then they fit perfectly in the allotted space of either NaCl (5.6 Å) or NaBr (5.96 Å). However, neither the Eu-Mn nor the Pb-Mn pair fit well in the allotted space of the KCl lattice (6.28 Å). Therefore, the formation of these pairs is expected to be less favorable in the latter crystal than in any of the sodium halides. This fact has been also confirmed recently by Capelletti and co-workers<sup>6</sup> studying the  $\text{Eu}^{2+} \rightarrow \text{Mn}^{2+}$  energy-transfer mechanisms which are active in the  $\text{KCl}:\text{Eu}^{2+}, \text{Mn}^{2+}$  system.

In order to obtain additional information which may give support to the ionic-radius criterion to predict pairing between doubly valent impurity ions in an alkali halide host, in the present work a study of  $\text{Sn}^{2+}$ -sensitized  $\text{Mn}^{2+}$  fluorescence in monocrystalline NaCl has been carried out. Tin was selected to perform this investigation since the optical absorption and emission spectra of this ion in NaCl have been previously characterized as a function of concentration, as well as of several thermal treatments given to the crystals.<sup>7</sup> Moreover, its ionic radius (0.93 Å) is quite appropriate to make a useful comparison with the data obtained in NaCl doubly doped with either europium and manganese or lead and manganese ions.

## II. EXPERIMENT

Single crystals of NaCl doped with tin or doubly doped with tin and manganese ions were grown in our laboratory by the Bridgman technique. The concentration of tin in the samples employed was estimated from the *C* band in the optical-absorption spectrum of the freshly quenched crystals using Smakula's equation with a value for the oscillator strength equal to 1.<sup>8</sup> Manganese concentration was determined by atomic absorption spectrophotometry. Thermal quenching was carried out by heating the samples for 1 h at 870 K and then dropping them as fast as possible onto a massive copper block at room temperature.

Continuous fluorescence measurements were carried out with a Perkin Elmer model 650-10-S spectrofluorimeter which was equipped with a 150-W xenon lamp and a red-sensitive Hamamatsu R-928 photomultiplier tube. Some of the emission spectra were obtained with a Perkin Elmer model LS-5 spectrofluorimeter which was operated in either the fluorescence or the phosphorescence mode in order to clearly characterize the emissions of tin and manganese. In all cases, the emission and excitation spectra were corrected for lamp intensity and photomultiplier sensitivity. Optical-absorption spectra were taken with a Perkin Elmer  $\lambda$ -5 double-beam recording spectrophotometer.

Lifetime data were obtained by exciting the samples at 266 nm with 30-ps pulses of a quadrupled Nd:YAG (yttrium aluminum garnet) laser at the laboratory of R. C. Powell at Oklahoma State University. The sample fluorescence was detected by an RCA C-31034 photomultiplier tube via a McPherson 0.45-m Czerny-Turner monochromator. The electrical signal of the phototube was processed by either a PAR model 165 gated integrator connected to a PAR model 162 boxcar averager or by a Tektronix model 7104 storage oscilloscope. For the low-temperature measurements the sample was mounted in the cold finger of an air-products model CS-202 cryogenic refrigerator with a temperature controller capable of temperature variation between 11 and 300 K.

## III. RESULTS

### A. NaCl:Sn<sup>2+</sup> samples

The room-temperature absorption spectrum of a quenched sample of NaCl containing 28 ppm of Sn<sup>2+</sup> ions is portrayed in Fig. 1. It consists of three structured bands labeled *A*, *B*, and *C* in increasing order of energy. These bands are due to electronic transitions<sup>8,9</sup> of the Sn<sup>2+</sup> ions associated with the change in configuration  $s^2 \rightarrow sp$ ; the *A* band has been attributed to the spin-orbit allowed transition  $|^1A_{1g}\rangle \rightarrow -\nu|^1T_{1u}\rangle + \mu|^3T_{1u}\rangle$ , where  $\mu$  and  $\nu$  are the mixing coefficients for the  $|^3T_{1u}\rangle$  and  $|^1T_{1u}\rangle$  states; the *B* band to the forbidden transitions  $|^1A_{1g}\rangle \rightarrow|^3T_{2u}\rangle$  and  $|^1A_{1g}\rangle \rightarrow|^3E_{1u}\rangle$  and the *C* band to the transition  $|^1A_{1g}\rangle \rightarrow -\mu|^1T_{1u}\rangle$

$+ \nu|^3T_{1u}\rangle$ .

When the crystals were illuminated with light lying within either of the *A*, *B*, or *C* bands luminescence was observed. Figure 2(a) shows, as an example, the obtained emission spectrum when the excitation was performed at 266 nm and for two selected sample temperatures. A similar spectrum was found when the excitation was performed with light lying in the wavelength range 230–320 nm. The room-temperature spectrum consists of a broad band peaking at 440 nm. When the sample temperature was lowered to 77 K, the width of the 440-nm band decreased considerably and another band peaking at 530 nm became apparent in the emission spectrum. This latter band was hardly detectable in the slightly tin-doped crystals (< 15 ppm) after a quenching treatment. The intensity ratio between the 530- and 440-nm bands was found to increase with tin concentration, as well as with the room-temperature storage of the freshly quenched crystals. For a tin concentration of  $\sim 150$  ppm, the intensities of both bands were found to be comparable in the emission spectrum of the quenched crystals; all these results being in good agreement with previous data.<sup>7</sup>

Although several models have been proposed to explain the origin of these two tin emission bands, the situation is far from being clear. While Zazubovich<sup>10–13</sup> and co-workers attributed these bands to the coexistence of different types of isolated Sn<sup>2+</sup> cation vacancy centers (i.e., the 440-nm band was ascribed to tin ions associated with a next nearest-neighbor cation vacancy and the 530-nm band with the tin ions associated with a nearest-neighbor cation vacancy), Fukuda<sup>14–16</sup> proposed that these two emissions are due to transitions from the two kinds of minima ( $A_T$  and  $A_X$ ) on the adiabatic-potential-energy surface (APES) of the  $^3T_{1u}$  relaxed excited state of the isolated tin ions which are forming the Sn<sup>2+</sup> cation vacancy dipoles. The coexistence of these two minima was attributed<sup>8,14</sup> to the quadratic Jahn-Teller effect and/or anharmonicity or to spin-orbit mixing between the excited states  $^3T_{1u}$  and  $^1T_{1u}$ . On the other hand, Marculescu *et al.*<sup>7</sup> proposed that the origin of these two bands could be alternatively explained considering that the  $A_T$  (440 nm) emission is produced by deexcitation of a tin center in the  $^3T_{1u}$  state while the  $A_X$  (530 nm) emission is produced by deexcitation of a different tin center which reached the excited state  $^1T_{1u}$  through a resonant energy-transfer process from a tin center in the excited state  $^3T_{1u}$ . Moreover, since the intensity of the 530-nm band is enhanced with the increase in tin concentration, as well as with the room-temperature storage of the samples, it is suggested that this emission is related in some way to tin aggregated complexes which are formed as a result of the aging at 300 K or because the tin concentration in the crystal is above the solubility limit.

In view of this situation and because the presence of a significant concentration of tin aggregates in the samples analyzed might complicate the interpretation of the results obtained, all the data reported in the next section were taken on slightly tin-doped crystals for which the emission peaking at 530 nm was hardly detectable even under very high-resolution conditions of our experimental setup.

### B. NaCl:Sn,Mn samples

The absorption spectrum of a tin (4 ppm) and manganese (30 ppm) doubly doped quenched crystal of NaCl was found to be nearly identical to that portrayed in Fig. 1 for the tin-doped NaCl. Light absorption in either of the *A*, *B*, or *C* bands produced an emission which is shown in Fig. 2(b) for two selected sample temperatures. At both temperatures the emission spectrum consisted of only two broad bands situated in the blue and red regions of the electromagnetic spectrum. The blue emission had the same characteristics (peak position and width) of the tin-emission band peaking at 440 nm in NaCl:Sn and therefore, was related with the deexcitation of the tin ions in our doubly doped quenched crystals. On the other hand, the red emission was observed only after the NaCl:Sn crystal was contaminated with manganese ions. The peak position of this emission was found to shift to the red region of the electromagnetic spectrum when the sample temperature was lowered. Both the peak energy and shift with temperature of this emission are consistent with the  $Mn^{2+}$  emission characteristics. Moreover, the introduction of manganese ions into the tin-doped NaCl crystals produced a reduction in the integrated intensity of the tin emission.

The liquid-nitrogen excitation spectra for the emission bands peaking at 440 and 600 nm are portrayed in Fig. 3. In all cases, the intense excitation bands are due to  $Sn^{2+}$  transitions.

Lifetime measurements were carried out in the range of temperatures 11–300 K on the tin and manganese emission transitions peaking at 440 and 580–620 nm, respectively. The very small intensity of the tin emission peaking at 530 nm in all the samples analyzed did not allowed us to obtain accurate lifetime data for this emission. In the temperature range investigated the manganese fluorescence decay exhibited a purely exponential time dependence with a no observable rise time. The time

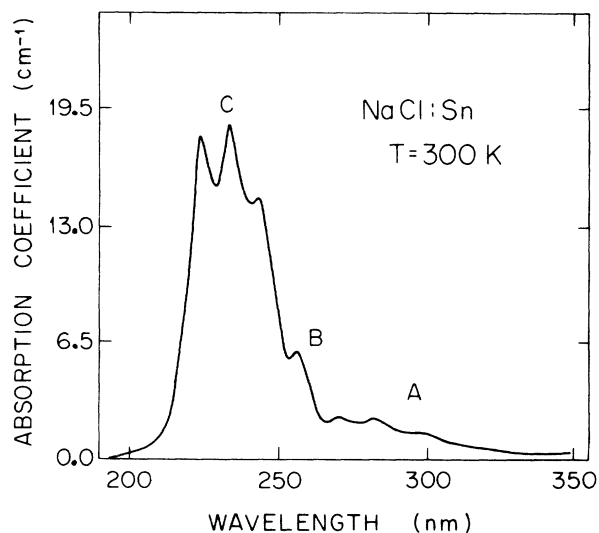


FIG. 1. Room-temperature absorption spectrum for a freshly quenched crystal of NaCl containing 28 ppm of  $Sn^{2+}$  ions.

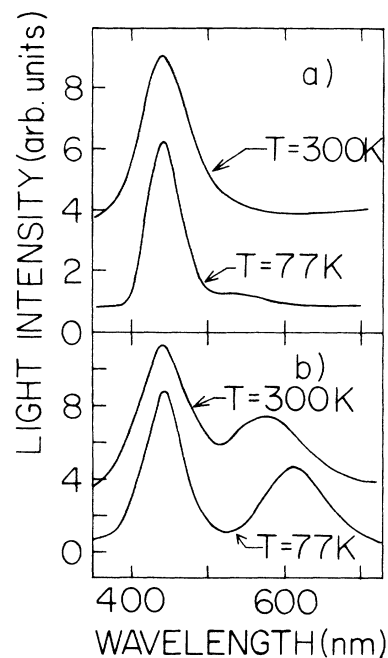


FIG. 2. (a) Emission spectra for  $Sn^{2+}$  in NaCl at two selected sample temperatures. This spectrum was taken on the same sample from which the absorption spectrum given in Fig. 1 was obtained. (b) Emission spectra for a tin and manganese doubly doped quenched crystal of NaCl when the excitation is performed at 266 nm.

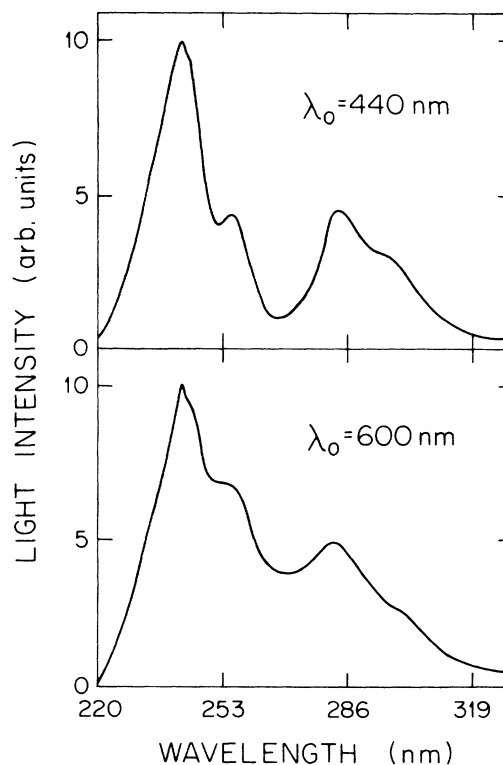


FIG. 3. Liquid-nitrogen excitation spectra for the emission bands peaking at 440 and 600 nm.

constant of the decay which corresponds to the lifetime of the  ${}^4T_{1g}(G)$  excitation level of  $Mn^{2+}$  increased from 18.5 ms at room temperature to 37 ms at 11 K. The tin fluorescence peaking at 440 nm also consisted of a unique decay constant which increased from 2.3  $\mu s$  at room temperature to 29  $\mu s$  at 11 K unlike the nonexponential decays usually observed for ion-ion energy transfer in solids. On the other hand, the  $Sn^{2+}$  fluorescence peaking at 440 nm in a sample having no manganese present also exhibited a pure exponential decay with a lifetime which was determined to be equal, within experimental error ( $\pm 5\%$ ), to that measured for the  $Sn^{2+}$  emission in the doubly doped crystals.

It was also ascertained that the aging at room temperature for several months did not produce a significant change in either the intensity of the tin emission or of the manganese one. This result might be expected considering that for the low concentrations of donor and acceptor ions in our samples it is quite certain that the room-temperature solubility limit of these impurities has not been exceeded. Therefore, impurity aggregates and/or precipitates are not expected to be formed during the room-temperature annealing.

#### IV. DISCUSSION

The more significant experimental data described above can be summarized as follows.

(1) Room-temperature excitation of the  $Sn^{2+}$  ions in our slightly doped  $NaCl:Sn^{2+}(4 \text{ ppm}), Mn^{2+}(30 \text{ ppm})$  samples produced two emission bands at peaking at 440 and 580 nm. The former band is due to the deexcitation of the tin ions, while the latter is due to the transition  ${}^4T_1(G) \rightarrow {}^6A_1$  of the  $Mn^{2+}$  ions. The peak position of this band moves to the red when the sample temperature decreases because of an increase in the magnitude of the crystal field acting at the site occupied by the manganese ions. On the other hand, the decrease in the lifetime of this emission when the sample temperature is increased may be explained considering that the probabilities for the phonon-assisted and nonradiative processes are enhanced with the increase in temperature.

(2) The excitation spectrum of the  $Mn^{2+}$  luminescence reveals the presence of the  $Sn^{2+}$  absorption bands. This result clearly indicates that  $Sn^{2+} \rightarrow Mn^{2+}$  energy transfer takes place in our doubly doped quenched samples of NaCl. This process occurs even for the very low concentrations of the donor and activator ions in our crystals.

(3) Pulse excitation of  $Sn^{2+}$  resulted in a  $Mn^{2+}$  luminescence with no observable rise time. Taking into account the sensitivity and the overall time response of our experimental setup, this result indicated that the rise time of the manganese fluorescence was shorter than 25 ns.

(4) The decay pattern of the  $Sn^{2+}$  luminescence in  $NaCl:Sn$  is *not affected* by the presence of manganese ions in the doubly doped crystals.

(5) The total integrated emission of the  $Sn^{2+}$  ions is reduced by the presence of the manganese ions.

The  $Sn^{2+}$  emission overlaps considerably the  $Mn^{2+}$  ab-

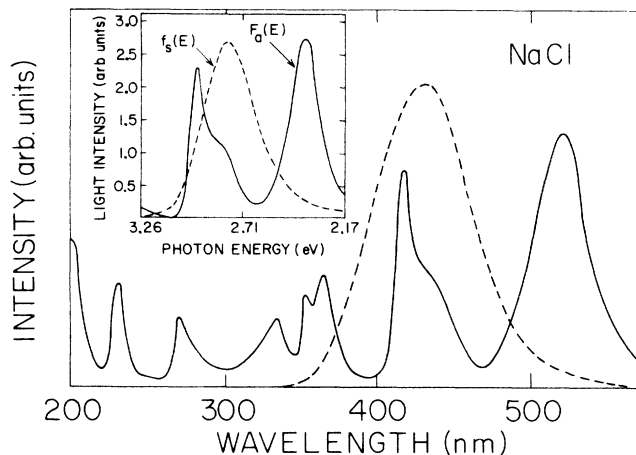


FIG. 4. Room-temperature overlap region of the tin emission (dashed line) and manganese absorption (solid line). The latter spectrum was taken from the work of Rodriguez *et al.* (Ref. 23). The inset in this figure shows the normalized line-shape functions in the overlap region.

sorption as can be appreciated from the spectra portrayed in Fig. 4. This spectral overlap is a necessary condition for the occurrence of  $Sn^{2+} \rightarrow Mn^{2+}$  energy transfer. However, for the low concentrations of the impurities in our samples, the interaction distance between donors and acceptors calculated from a truly random distribution of the impurities is found to be  $> 100 \text{ \AA}$ . At this large interaction distance energy transfer between the impurities should not have occurred in our doubly doped quenched crystals. In fact, the rate of  $Sn \rightarrow Mn$  energy transfer calculated from Dexter's theory<sup>17</sup> of energy transfer, at a distance of  $\sim 100 \text{ \AA}$ , is found to be quite small compared with the experimentally determined decay rate of the  $Sn^{2+}$  ions. Therefore, the observation of tin-sensitized manganese fluorescence in our samples suggests that the impurities are not randomly distributed in the lattice but rather occur as coupled pairs of  $Sn^{2+}-Mn^{2+}$ . A nearest-neighbor cation separation distance ( $\sim 5.6 \text{ \AA}$ ) in the NaCl lattice along the [100] direction predicts a very efficient energy transfer, as it will be shown below.

On the basis of these observations, a model which may describe the essential features of the kinetics of  $Sn \rightarrow Mn$  energy transfer in the lattice of NaCl can be built up. In this model, which is depicted in Fig. 5, both the sensitizer-tin and activator-manganese ions are treated as two energy-level systems. In particular, in order to incorporate observations 4 and 5 this model considers that for coupled  $Sn^{2+}-Mn^{2+}$  ions the energy transfer from the tin to the manganese ions proceeds at a rapid rate that quenches the sensitizer luminescence completely. On the other hand, the unpaired tin ions are, on the average, at a distance from the manganese ions such that no energy transfer can take place, leaving therefore the lifetime of the donor ions unchanged. According to this situation, the tin ions which are paired with the manganese ions do not exhibit any fluorescence and the observed tin emission originates *exclusively* from the ions which are not in-

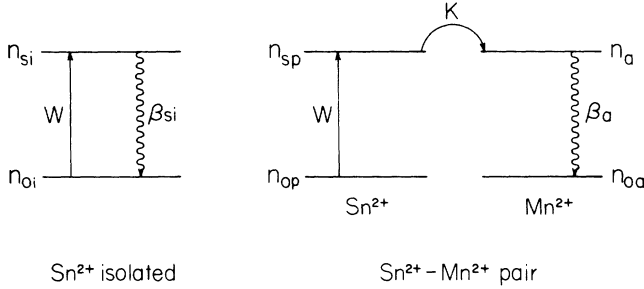


FIG. 5. Energy-level system used to describe the kinetics of tin-manganese energy transfer in the lattice of NaCl.

interacting with  $\text{Mn}^{2+}$ . Moreover, the observed red emission is due to the  ${}^4T_1(G) \rightarrow {}^6A_1$  transition of  $\text{Mn}^{2+}$  which results from excitation by energy transfer from the tin ions forming the impurity pairs.

According to this model, the rate equations describing the time evolution of the excited-state populations of both isolated tin ions and Sn-Mn pairs are given by

$$\begin{aligned} \frac{dn_{si}}{dt} &= wn_{oi} - \beta_{si}n_{si}, \\ \frac{dn_{sp}}{dt} &= wn_{op} - Kn_{sp}, \\ \frac{dn_a}{dt} &= Kn_{sp} - \beta_a n_a, \end{aligned} \quad (1)$$

where  $n_{si}$  and  $n_{sp}$  are the populations of the excited states of the Sn ion when it is in the isolated and in the coupled form, respectively,  $n_{oi}$  and  $n_{op}$  are the corresponding populations for the ground state,  $n_a$  is the concentration of the excited state of the manganese ions forming the impurity pairs,  $\beta_{si}$  and  $\beta_a$  are the fluorescence decay rates of the isolated tin and coupled manganese ions,  $K$  is the rate of energy transfer, and  $w$  is the absorption probability which has been assumed to be the same for both isolated and coupled tin ions. Direct excitation of  $\text{Mn}^{2+}$  has been considered to be negligible in view of the forbidden nature of the  $d \rightarrow d$  absorption transitions.

Taking into account that the isolated pair transfer rate is time independent,<sup>18</sup> solutions to the rate equations can be obtained under the assumption of a  $\delta$ -function excitation pulse:

$$\begin{aligned} n_{si}(t) &= n_{si}(0) \exp(-\beta_{si}t), \\ n_a(t) &= \frac{-Kn_a(0)}{(\beta_a - K)} [\exp(-Kt) + \exp(-\beta_a t)]. \end{aligned} \quad (2)$$

Now, the intensity of the activator ions reaches a maximum value after pulse excitation of the donor ions at a time  $t_{\max}$  given by

$$t_{\max} = \frac{1}{(K - \beta_a)} \ln(K/\beta_a). \quad (3)$$

From Eq. (3) and our experimentally determined data, i.e.,  $t_{\max} < 25$  ns and  $\beta_a = 54$  s<sup>-1</sup>, the rate of  $\text{Sn}^{2+} \rightarrow \text{Mn}^{2+}$  energy transfer was estimated to be

$> 3 \times 10^8$  s<sup>-1</sup> at 300 K.

Considering the forbidden nature of the  $3d \rightarrow 3d$   $\text{Mn}^{2+}$  absorptions, it is expected that the Sn  $\rightarrow$  Mn energy-transfer mechanism which takes place between these two impurity ions in NaCl is either of the electric dipole quadrupole type or exchange in nature. According to Dexter's theory,<sup>17</sup> the transfer rate for the electric dipole-quadrupole interaction is given by

$$w_{sa}^{DQ} = \frac{3\hbar^4 c^4 f_q}{4\pi n^4 \tau_s^0 f_d} (\lambda_s)^2 \left[ \frac{1}{R_{sa}} \right]^8 Q_a \int \frac{f_s(E) F_a(E)}{E^4} dE, \quad (4)$$

where  $\tau_s^0$  and  $\lambda_s$  are the intrinsic lifetime (in the absence of energy transfer) and the wavelength position of the sensitizer's emission,  $R_{sa}$  is the interaction distance between the ions involved in the transfer,  $Q_a$  is the integrated absorbance of the acceptor ion,  $E$  is the energy involved in the transfer, and  $f_q$  and  $f_d$  are the oscillator strengths of the activator quadrupole and dipole electrical transitions. The integral  $\Omega = \int [f_s(E) F_a(E)/E^4] dE$  represents the spectral overlap between the normalized shapes of the tin emission [ $f_s(E)$ ] and manganese absorption [ $F_a(E)$ ]. The other symbols in Eq. (4) have their usual meaning.

Since the absorption coefficient of manganese is quite difficult to measure,  $Q_a$  was estimated following the procedure described previously;<sup>4</sup> the result being  $Q_a = 4.8 \times 10^{-23}$  eV cm<sup>2</sup>. The overlap integral was calculated using the room-temperature tin emission and the manganese absorption spectra portrayed in Fig. 4. The normalized line-shape functions for the Sn emission and Mn absorption in the overlap region are shown in the inset of the same figure. The value of  $\Omega$  was found to be  $3.4 \times 10^{-2}$  eV<sup>-5</sup>.

Now, using the fluorescence decay data for the tin emission and the values for  $Q_a$  and  $\Omega$  mentioned above, the critical interaction distance  $R_0$  defined as the distance at which  $w_{sa}^{DQ} \tau_s^0 = 1$  can be estimated from Eq. (4); the result being  $\sim 10$  Å at 300 K. On the other hand, since the exact nature of the Sn-Mn pair cannot be inferred from our experimentally determined data, the rate of energy transfer via a dipole-quadrupole interaction mechanism was calculated using different configurations for the Sn-Mn dimer complex such as those given in Fig. 6. Defect and binding energies for these types of dimers have been calculated for different kinds of doubly valent impurity ions in the alkali halides by Bannon *et al.*<sup>19</sup> using computer simulation techniques based on generalized Mott and Littleton methods. The obtained values for  $w_{sa}^{DQ}$  for each of the considered dimer complexes are given in Table I. In the same Table, the rate of energy transfer calculated from the use of an electric dipole-dipole interaction mechanism is also included for the sake of comparison. As expected, more reasonable values are obtained when a dipole-quadrupole interaction mechanism is employed rather than an electric dipole-dipole one. Moreover, the closer agreement between the calculated values for  $w_{sa}^{DQ}$  and that estimated experimentally is achieved when the [100] dimer configuration ( $D_1$ ) is employed to perform the calculations. The calculated value, however, is still

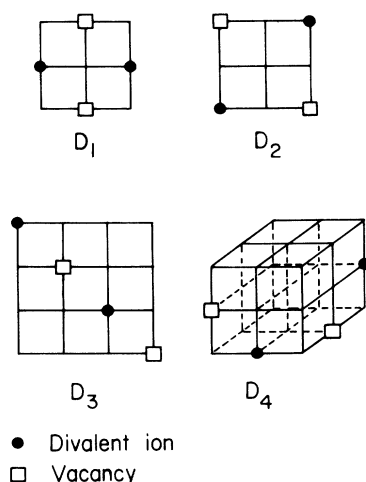


FIG. 6. Possible configurations for the Sn-Mn dimer complex in the lattice of NaCl which were considered in order to calculate the rate of energy transfer via multipolar or exchange interaction mechanisms.

smaller than that estimated from our experimental data. This fact may suggest that an exchange (superexchange) interaction mechanism is probably the responsible for the energy transfer from the tin to the manganese ions forming the impurity pairs. Such interaction can lead to energy-transfer rates much higher than those predicted from Eq. (4). In fact, magnetic studies have shown<sup>20</sup> that exchange between cations can be relatively strong for 180° interactions involving one  $p$  orbital of an anion intermediary, as it occurs in the  $D_1$  dimer configuration.

Unfortunately, neither the probability for energy transfer nor the critical interaction distance can be calculated precisely for an exchange interaction mechanism since both quantities are strongly dependent on the wave-function overlap integral of the sensitizer and activator electrons involved in the interaction. This makes it important to use accurate expressions for the wave functions which are not known. However, a rough estimation of the magnitude of this interaction can be obtained from the expression derived by Dornauf and Heber<sup>21</sup> for the transfer probability in the case of superexchange

$$w_{sa}^{se} = \frac{1}{\tau_s^0} \exp[\gamma(R_0 - R_{sa})], \quad (5)$$

where  $\tau_s^0$ ,  $R_0$ , and  $R_{sa}$  have the same meaning as above

TABLE I. Theoretical calculated values for the rate of energy transfer from tin to manganese ions in NaCl at 300 K using the dimer configurations show in Fig. 6.

Dimer configuration	Sensitizer-activator distance (Å)	Energy-transfer rate	
		$w_{sa}^{DD}$ ( $s^{-1}$ )	$w_{sa}^{DQ}$ ( $s^{-1}$ )
$D_1$	5.6	$8.0 \times 10^4$	$0.5 \times 10^8$
$D_2, D_3$	7.9	$1.0 \times 10^4$	$3.1 \times 10^6$
$D_4$	6.8	$2.4 \times 10^4$	$9.8 \times 10^6$

and  $\gamma$  is the exchange constant. According to Dexter<sup>17</sup>  $\gamma$  is equal to  $2/L$  where  $L$  is an “effective average Bohr radius” for the excited and unexcited states of the complex involved. Using the  $D_1$  dimer configuration, a value for  $R_0$  similar to that found for the dipole-quadrupole interaction mechanism and a typical value for the “effective Bohr radius” of 1.3 Å which is about half the manganese-chlorine separation distance in this dimer configuration, a rate of  $0.3 \times 10^9 s^{-1}$  is obtained. If we juxtapose this result to the  $w_{sa}^{DQ}$  calculated above, we may conclude that Sn→Mn energy transfer via a superexchange interaction mechanism appears to have a higher probability than Sn→Mn energy transfer via a multipolar interaction mechanism. Unfortunately an estimation for the rate of energy transfer via an exchange mechanism is not simple for the case in which the impurities are forming the other dimer configurations as those shown in Fig. 6. However, the large distances between doner and acceptor ions, as well as their locations in these complexes appear to be unappropriated for the occurrence of this type of interaction.

Although it is recognized that these type of calculations are phenomenological, they may suggest that the possible nature of the Sn-Mn complex could be that of the  $D_1$  dimer. They also indicate that the experimental data can only be plausibly explained if a short-range interaction mechanism of energy transfer is active between the tin and manganese ions forming the impurity pairs in the lattice of NaCl.

Let us now consider the model predictions for the relative integrated fluorescence intensities of the isolated tin and coupled manganese ions. Equations (1) can be easily solved for continuous excitation to give the steady-state populations:  $n_{si} = wn_{oi}/\beta_{si}$  and  $n_a = wn_{op}/\beta_a$ . Since the fluorescence intensity of a specific level is equal to the product of the population and the radiative decay rate ( $\beta'$ ) of the level, the ratio for the emission intensities of the activator manganese ions ( $I_a$ ) and the isolated tin ions ( $I_{si}$ ), in the limit of weak pumping where  $n_{oi} \approx N_{si}$  and  $n_{op} \approx N_{sp}$  is given by

$$I_a/I_{si} = [(\beta'_a/\beta_a)N_{sp}] / [(\beta'_{si}/\beta_{si})N_{si}], \quad (6)$$

where  $N_{si}$  and  $N_{sp}$  are the total concentrations of isolated and coupled tin ions.

The ratio for the number of tin ions which are paired with the manganese ions ( $N_{sp}$ ) and the total concentration of tin ( $N_{st} = N_{si} + N_{sp}$ ) in the crystal can be obtained from Eq. (6) after some minor manipulations:

$$\frac{N_{sp}}{N_{st}} = \frac{I_a(\beta'_{si}/\beta_{si})}{I_{si}[\beta'_a/\beta_a + (I_a/I_{si})\beta'_{si}/\beta_{si}]} \quad (7)$$

Considering that the radiative decay rates are equal to the inverse of the low-temperature (11 K) lifetime values ( $\beta'_{si} = 3.4 \times 10^4 s^{-1}$ ;  $\beta'_a = 27 s^{-1}$ ),  $N_{sp}/N_{st}$  is found to be  $\sim 0.05$  when our experimentally determined room-temperature data, i.e.,  $\beta_{si} = 4.3 \times 10^5 s^{-1}$ ,  $\beta_a = 54 s^{-1}$ , and  $I_a/I_{si} \cong 0.3$  are employed in Eq. (7). Thus, about 5% of the total concentration of the  $Sn^{2+}$  ions in our doubly

doped quenched crystals are paired with the manganese ions.

It is important to mention that previous data<sup>22</sup> on KCl:Sn<sup>2+</sup> revealed that the lifetime of the tin emission in this crystal increases by about an order of magnitude when the sample temperature was lowered from 11 to 4 K. If a similar increase in the tin-emission lifetime occurs in NaCl when the sample temperature is decreased from 11 to 4 K, then the calculated value for the radiative rate of the tin emission will be  $\sim 10^3$  rather than  $\sim 10^4$ . When this lower value for  $P_{Sn}^r$  is used in Eq. (7), it is found that  $N_{sp}/N_{st} \cong 5 \times 10^{-3}$ . Since we are not able to lower the sample temperature below 11 K and determine whether or not an increase in the lifetime of the tin emission also occurs in NaCl, it might be possible that the calculated percentage of paired tin ions from Eq. (7) could be smaller.

At this point, it should be pointed out that in our previous works<sup>2,4</sup> dealing with the energy transfer from europium to manganese ions in NaCl and NaBr, the number of europium ions which was paired with the manganese ions was estimated to be over 90% in both cases. This percentage is overestimated since it was obtained from the use of a quite simplified procedure which is not correct in order to describe the whole essential features of the isolated and the impurity pair system. In fact, if the kinetics of Eu  $\rightarrow$  Mn energy transfer in these crystals are treated with a model similar to that depicted in Fig. 5, then the percentage of europium ions which are associated with manganese is calculated from our experimentally determined data to be  $\sim 35$ , 27, and 0.2 in NaCl, NaBr, and KCl, respectively. Although, these percentages are much smaller than those estimated previously, they still point out to the strong tendency of the Eu<sup>2+</sup> and Mn<sup>2+</sup> ions to form close pairs in the sodium halide lattices.

A comparison of the data obtained in the systems NaCl:Eu,Mn and NaCl:Sn,Mn shows that in both crystals impurity pairs are formed. However, the Eu-Mn pairs are more numerous than the Sn-Mn pairs. This result is in agreement with the ionic radius criterion. In fact, the average radius (0.96 Å) of the Eu<sup>2+</sup> and Mn<sup>2+</sup> ions is more similar to that of the host cation sodium ions (0.99 Å) than that of the Sn<sup>2+</sup> and Mn<sup>2+</sup> ions (0.87 Å). Therefore, according to this criterion, the formation of Eu-Mn pairs will be more favorable than that of Sn-Mn in the lattice of NaCl.

Finally, experiments are now in progress in order to determine if Sn-Mn pairs are also formed in the slightly doped quenched crystals of KCl. This determination might be a significant one in order to test even more the validity of the ionic radius criterion to predict pairing between two doubly valent impurity ions in an alkali halide host. It will be also very interesting to determine whether or not this criterion is appropriate to predict pairing between a monovalent and a doubly valent impurity ion in the alkali halides.

#### ACKNOWLEDGMENTS

This work was partially supported by Secretaría de Educación Pública and Consejo Nacional de Ciencia y Tecnología under Contracts No. C86-01-0258 and No. PCEXCNA-040394, respectively. We would like to express our appreciation to Professor R. C. Powell for putting at our disposal his laboratory and to Dr. Andrzej Suchocki for helping us to perform the pulse excitation measurements. The technical assistance of I. Camarillo is gratefully acknowledged. We also thank C. Garza for determining manganese concentration in the crystals employed by atomic absorption spectrophotometry.

<sup>1</sup>M. D. Shinn and W. A. Sibley, *Phys. Rev. B* **29**, 3834 (1984).

<sup>2</sup>J. Rubio O., H. Murrieta S., R. C. Powell, and W. A. Sibley, *Phys. Rev. B* **31**, 59 (1985).

<sup>3</sup>J. Rubio O., C. Marin, J. Hernandez A., J. Garcia M., and H. Murrieta S., *J. Phys. C* **20**, 1173 (1987).

<sup>4</sup>J. Rubio O., A. Muñoz F., and J. Garcia M., *Phys. Rev. B* **36**, 8115 (1987).

<sup>5</sup>J. Rubio O., A. Muñoz F., C. Zaldo, and H. Murrieta S., *Solid State Commun.* **65**, 251 (1988).

<sup>6</sup>R. Capelletti, M. Manfredi, R. Cywinski, J. Z. Damm, E. Mugenski, and M. Solzi, *Phys. Rev. B* **36**, 5124 (1987).

<sup>7</sup>L. Marculescu, G. Ghita, and L. Mihut, *Phys. Status Solidi. A* **61**, 497 (1980).

<sup>8</sup>A. Ranfagni, D. Mugnai, M. Bacci, G. Viliani, and M. Fontana, *Adv. Phys.* **32**, 823 (1983), and references cited therein.

<sup>9</sup>A. Fukuda, *Sci. Light (Tokyo)* **13**, 64 (1964).

<sup>10</sup>E. A. Vasilichenko, S. G. Zazubovich, and H. E. Luschik, *Opt. Spectrosk.* **32**, 749 (1972).

<sup>11</sup>E. Realo and S. G. Zazubovich, *Phys. Status Solidi. B* **57**, 69 (1973).

<sup>12</sup>S. G. Zazubovich, *Opt. Spectrosk.* **37**, 711 (1974).

<sup>13</sup>V. Hizhnyakov and S. G. Zazubovich, *Phys. Status Solidi. B* **86**, 733 (1978).

<sup>14</sup>A. Fukuda, *Phys. Rev. B* **1**, 4161 (1970).

<sup>15</sup>A. Fukuda, *Phys. Rev. Lett.* **26**, 314 (1971); *ibid.* **28**, 1032 (1972).

<sup>16</sup>A. Fukuda, *Solid. State. Commun.* **12**, 1039 (1973).

<sup>17</sup>D. L. Dexter, *J. Chem. Phys.* **21**, 836 (1953).

<sup>18</sup>R. C. Powell and G. Blasse, in *Structure and Bonding*, edited by J. D. Dunitz, J. B. Goodenough, P. Hemmerich, J. A. Ibers, C. K. Jorgensen, J. B. Neilands, D. Reinen, and R. J. P. Williams (Springer, Berlin, 1980); M. J. Treadaway and R. C. Powell, *Phys. Rev. B* **11**, 862 (1975).

<sup>19</sup>N. M. Bannon, J. Corish, and P. W. M. Jacobs, *Philos. Mag.* **A 6**, 797 (1985).

<sup>20</sup>P. W. Anderson, in *Magnetism*, edited by G. T. Rado and H. Suhl (Academic, New York, 1963), Vol. 1.

<sup>21</sup>H. Dornauf and J. Heber, *J. Lumin.* **22**, 1 (1980).

<sup>22</sup>V. Hizhnyakov, S. Zazubovich, and T. Soovik, *Phys. Status Solidi B* **66**, 727 (1974).

<sup>23</sup>F. Rodriguez, M. Moreno, F. Jaque, and F. J. Lopez, *J. Chem. Phys.* **78**, 73 (1983).